online data

Characterization of unique amphipathic antimicrobial peptides from venom of the scorpion *Pandinus imperator*

Gerardo CORZO*[1], Pierre ESCOUBAS*[2], Elba VILLEGAS†, Kevin J. BARNHAM‡, Weilan HE‡, Raymond S. NORTON‡[3] and Terumi NAKAJIMA*

*Suntory Institute for Bioorganic Research, Mishima-Gun, Shimamoto-Cho, Wakayamadai 1-1-1, Osaka 618-8503, Japan, †Suntory Institute for Fundamental Research, Mishima-Gun, Shimamoto-Cho, Yamazaki 5-2-5, Osaka 618-0001, Japan, and ‡Biomolecular Research Institute, 343 Royal Parade, Parkville 3052, Australia

Two novel antimicrobial peptides have been identified and characterized from venom of the African scorpion *Pandinus imperator*. The peptides, designated pandinin 1 and 2, are α-helical polycationic peptides, with pandinin 1 belonging to the group of antibacterial peptides previously described from scorpions, frogs and insects, and pandinin 2 to the group of short magainin-type helical peptides from frogs. Both peptides demonstrated high antimicrobial activity against a range of Gram-positive bacteria (2.4–5.2 μM), but were less active against Gram-negative bacteria (2.4–38.2 μM), and only pandinin 2 affected the yeast *Candida albicans*. Pandinin 2 also demonstrated strong haemolytic activity (11.1–44.5 μM) against sheep erythrocytes, in contrast with pandinin 1, which was not haemolytic. CD studies and a high-resolution structure of pandinin 2 determined by NMR, showed that the two peptides are both essentially helical, but differ in their overall structure. Pandinin 2 is composed of a single α-helix with a predominantly hydrophobic N-terminal sequence, whereas pandinin 1 consists of two distinct α-helices separated by a coil region of higher flexibility. This is the first report of magainin-type polycationic antimicrobial peptides in scorpion venom. Their presence brings new insights into the mode of action of scorpion venom and also opens new avenues for the discovery of novel antibiotic molecules from arthropod venoms.

Key words: α-helical peptides, arthropod venom, haemolytic activity.

INTRODUCTION

Polycationic antimicrobial peptides represent the chemical counterpart to the cell-mediated immune response in the innate host defense against pathogenic micro-organisms. Antimicrobial peptides have broad-spectrum non-specific activity against a wide range of micro-organisms, including viruses, Gram-positive and Gram-negative bacteria, protozoa, yeasts and fungi, and may also be haemolytic and cytotoxic to cancer cells [1,2]. Since their initial discovery [3], these peptides have been described in both vertebrates [4] and invertebrates [5], with a wide phylogenetic distribution, including humans [6]. They have been found in the skin, epithelial cells and blood of vertebrates, as well as in insect haemolymph and the venomous secretions of bees and wasps. They are relatively small (2–5 kDa), amphipathic and basic peptides of variable length, sequence and structure. Although there are divergent theories concerning their mechanism of action, they appear to form channels or pores in the cell membrane, inducing cell permeation and a breakdown of cellular physiology [7].

These peptides have been separated into two main categories according to whether or not they contain cysteine residues linked to form disulphide bridges. Currently, they are divided into four broad families based on their structures: (1) linear α-helical peptides represented by the cecropins, magainins and melittin, which adopt a random structure in dilute aqueous solution and form α-helices or a helix-bend-helix motif in organic solvents and upon contact with cell membrane phospholipids, (2) the proline- and arginine-rich apidaecins, which adopt an extended α-helical structure, (3) β-sheet peptides, which comprise the α- and β-defensins, and the protegrin/tachyplesin group, which contain several disulphide bridges, and adopt either a β-sheet or β-hairpin fold, sometimes associated with a short α-helix as in the scorpion defensins and (4) other antimicrobial peptides that are neutral or negatively charged and only partly α-helical, such as the bacteriocins, as well as large (>10 kDa) glycine-rich peptides. The number of antimicrobial peptides described has increased dramatically to more than 500, of which roughly half are linear α-helical peptides (http://bbcm1.univ.trieste.it/~tossi/pag1.htm).

Although many antimicrobial peptides have been described in insects [5], relatively few studies have addressed their presence in other arthropods. They occur in horseshoe crabs (*Limulus polyphemus*) [8] and also in arachnids. Magainin-type α-helical peptides have been described from venom of the wolf spider (*Lycosa carolinensis*) [9]. Another peptide was isolated from the venom of *Lycosa singoriensis* [10]. CsTX peptides from the venom of *Cupiennus salei* were also reported to have antimicrobial properties [11], although no primary structures are available yet. Gomesin, a cysteine-rich antimicrobial peptide with homology

Abbreviations used: CZE, capillary zone electrophoresis; DPC, dodecylphosphocholine; Fmoc, fluoren-9-ylmethoxycarbonyl; MALDI–TOF, matrix-assisted laser-desorption ionization–time-of-flight; MIC, minimal inhibitory concentrations; Pin1, pandinin 1; Pin2, pandinin 2; RP-HPLC, reversed-phase HPLC; TFA, trifluoroacetic acid; TFE, trifluoroethanol.

[1] To whom correspondence should be addressed (email corzo@sunbor.or.jp or corzev@hotmail.com).
[2] Present address: Institut de Pharmacologie Moleculaire et Cellulaire, CNRS, 660 route des Lucioles, Sophia Antipolis, 06560 Valbonne, France.
[3] Present address: NMR Laboratory, The Walter and Eliza Hall Institute of Medical Research, 381 Royal Parade, Parkville 3052, Australia.

with tachyplesin and polyphemusin from horseshoe crabs was recently isolated from haemolymph of the tarantula *Acanthoscurria gomesiana* [12].

Several antimicrobial peptides have been described from scorpions, including several cysteine-containing defensin-type peptides from haemolymph of the scorpions *Leiurus quinquestriatus hebraeus* [13] and *Androctonus australis* [14], buthinin, a three disulphide-bridge bactericidal and fungicidal peptide, and androctonin, a tachyplesin-type peptide with two disulphide bridges, from the venom of *Androctonus australis* [14], and scorpine, a 75-residue antimalarial peptide isolated from *Pandinus imperator* venom [15]. α-Helical peptides have also been reported from the venoms of *Hadrurus aztecus* (hadrurin) [16] and *Parabuthus schlechteri* (parabutoporin) [17]. In the present paper, we describe the isolation, chemical characterization, biological activity and structures of pandinins 1 and 2, two novel α-helical polycationic antimicrobial peptides from venom of the scorpion *P. imperator*. The discovery of these peptides in another scorpion venom confirms their widespread occurrence and significant biological function in venoms. Both peptides are potent antimicrobials, belong to distinct structural groups of α-helical antimicrobial peptides, and thus highlight important structural features regarding target selectivity and ability to interact with variously charged membranes. As only one peptide displays strong haemolytic activity, data on their structure and activity combined with that of other antimicrobial peptides can provide novel clues about structural features involved in membrane lysis. Pandinin 2 is the first representative of its class of antimicrobial peptides to be discovered in scorpion venom.

EXPERIMENTAL

Biological materials

P. imperator crude venom was obtained by electrical stimulation of the telson (post-segmental region of the abdomen) of scorpions kept in captivity. Magainin 1 was purchased from the Peptide Institute (Osaka, Japan). Trypsin (EC 3.4.21.4) and endoproteinase Glu-C (EC 3.4.21.19) were from Sigma (St. Louis, MO, U.S.A.). *P. imperato*r haemolymph was obtained by aseptic puncture of the dorsal tegument between mesosomal tergites VI and VII. The haemolymph was collected (1 ml) and immediately centrifuged to avoid coagulation. The supernatant and pellet were frozen until use. The microbial strains *Escherichia coli* (A.T.C.C. 11775), *Enterococcus faecalis* (A.T.C.C. 19433), *Bacillus subtilis* (A.T.C.C. 6051), *Candida albicans* (A.T.C.C. 18804), *Pseudomonas aeruginosa* (A.T.C.C. 10145), *Staphylococcus aureus* (I.A.M. 1098; Institute of Applied Microbiology Culture Collection, University of Tokyo) and *Staphylococcus epidermidis* (S.A.M. 0020; Suntory Applied Microbiology Culture Collection) were obtained from the Suntory Institute for Fundamental Research (Osaka, Japan).

Isolation of antimicrobial toxins

P. imperator crude venom (100 μl) was dissolved in 0.1 % aqueous trifluoroacetic acid (TFA) containing 5 % (v/v) acetonitrile, and the insoluble material was removed by centrifugation at 14000 ***g*** for 5 min. The supernatant was filtered through Millex-GV filters (0.45 μm) prior to fractionation. Diluted venom was initially fractionated using a reversed-phase semi-preparative C_{18} column (10 mm × 250 mm; Nacalai Tesque, Kyoto, Japan) equilibrated in 0.1 % TFA, and eluted with a linear gradient of acetonitrile/0.1 % TFA (0–60 % in 60 min) at a flow rate of 2 ml/min. Absorbance of the effluent was monitored at 215 nm. Fractions with antimicrobial activity were further fractionated by cation-exchange HPLC on a TSK-gel sulphopropyl column (7.5 mm × 75 mm; Tosoh, Tokyo, Japan), equilibrated in 0.5 M acetic acid, pH 2.9, and eluted with a linear gradient of 0.5 M acetic acid in 1 M ammonium acetate, pH 5.9 (0–100 % in 75 min), at a flow rate of 1 ml/min. The active fractions were finally purified on a reversed-phase C_4 column (4.6 mm × 250 mm; Nacalai Tesque) using the same gradient system as above at a flow rate of 1 ml/min.

Antimicrobial assays

Antimicrobial activity and minimal inhibitory concentrations (MIC) were assayed by determining the suppression of bacterial growth following application of HPLC fractions. *E. coli*, *B. subtilis* and all other bacterial strains were grown in liquid antibiotic 3-medium (Difco, Franklin Lakes, NJ, U.S.A.) for 18 h and 0.1 ml of bacterial suspension ($D_{600} = 0.3$–0.8) was diluted 1:100 in sterile antibiotic 3-medium. A 1 ml aliquot was then diluted 1:10 in warm (approx. 45 °C) antibiotic 3-medium containing 1.5 % (w/v) agar and the medium poured into 100 mm × 20 mm sterile Petri dishes. Depending on the strain, bacterial count was approx. 10^6–10^7 colony-forming units/ml. Vacuum-dried HPLC fractions were resuspended in 20 μl of distilled water and 5 μl was applied to the plate surface. Bacteria were incubated at 37 °C for 12–14 h and growth inhibition was detected as clear spots on the plate surface. Isolation of pandinin 1 and pandinin 2 was achieved following plate growth inhibition of *E. coli* and *B. subtilis*.

Erythrocyte haemolysis assay

Haemolytic activity was determined by incubating a 10 % (v/v) suspension of sheep erythrocytes with selected peptides. Erythrocytes were rinsed several times in 10 mM phosphate buffer, pH 7.2 (PBS), by centrifugation for 3 min at 3000 ***g*** until the *D* of the supernatant reached the *D* of the control (PBS only). Erythrocytes were then incubated at room temperature for 1 h in either deionized water (positive control), PBS (blank) or with the appropriate amount of pandinin 2 or magainin 1. The samples were then centrifuged at 10000 ***g*** for 5 min, the supernatant was separated from the pellet and absorbance measured at 570 nm. The relative *D* compared with that of the suspension treated with deionized water defined the percentage of haemolysis.

Sequence determination

Antimicrobial toxins were reduced with tributylphosphine (Nacalai Tesque) and alkylated with 4-vinylpyridine (Wako, Osaka, Japan) in 0.5 M $NaHCO_3$ buffer, pH 8.3, for 2 h at 37 °C in the dark prior to sequencing. As the molecular masses of the two antimicrobial peptides did not change after reduction and alkylation, they were directly sequenced on a Shimadzu PPSQ-10 automated gas-phase sequencer (Shimadzu, Kyoto, Japan). Toxins were dissolved in 30 μl of a 37 % acetonitrile solution and applied to TFA-treated glass-fibre membranes, precycled with polybrene (Aldrich, Milwaukee, WI, U.S.A.). Data were recorded on a Shimadzu CR-7A integrator.

The larger peptide, pandinin 1, was subjected to enzymic hydrolysis. Tryptic hydrolysis was carried out in 0.1 M sodium bicarbonate buffer, pH 8.1, at 37 °C for 3 h, using a 1:50 (w/w) enzyme-to-substrate ratio. Hydrolysis with type XVII-B endoproteinase Glu-C from *Staph. aureus* V8 was carried out in 0.1 M sodium bicarbonate buffer, pH 7.6, at 37 °C for 3 h, using a 1:20 (w/w) enzyme-to-substrate ratio. The tryptic and the endoproteinase Glu-C digests were fractionated by reversed-phase

HPLC (RP-HPLC) using a C_4 column (4.6 mm × 250 mm; Nacalai Tesque) and eluted with a linear gradient of acetonitrile in 0.1 % aqueous TFA. All fractions were analysed by matrix-assisted laser-desorption ionization–time-of-flight (MALDI–TOF) MS. All tryptic fragments, and the two major endoprotease Glu-C fragments, were sequenced by automated Edman degradation.

Mass spectrometry

MALDI–TOF mass spectra were obtained on Perseptive Voyager Elite and Voyager DE-Pro spectrometers (Applied Biosystems, Tokyo, Japan) using positive acceleration in either linear or reflector mode. Time-to-mass conversion in linear mode was achieved by external calibration using bradykinin (m/z 1061.2), bovine pancreatic β-insulin (m/z 3496.6) and bovine pancreatic insulin (m/z 5734.5) (Sigma) as standards or a peptide mixture as internal calibrants in reflector mode. All experiments were performed using α-cyano-4-hydroxycinnamic acid (Aldrich) as the matrix.

Peptide synthesis

Pandinin 1 and the two C-terminal forms of pandinin 2 were chemically synthesized by a solid-phase method using the fluoren-9-ylmethoxycarbonyl (Fmoc) methodology on an Applied Biosystems 433A peptide synthesizer. Fmoc-Thr(t-butyl)-Wang resin was used to provide a free carboxy group at the C-terminus of synthetic pandinin 1 (sPin1-OH) and an Fmoc-Asp(Ot-butyl)-Wang resin was used to provide a free carboxyl at the C-terminus of carboxylated synthetic pandinin 2 (sPin2-OH). A Rink amide 4-(2′,4′-dimethoxyphenyl-Fmoc-aminomethyl)phenoxy resin was used to provide the amino group at the C-terminus of the amidated synthetic pandinin 2 (sPin2-NH_2). After chemical synthesis, cleavage and deprotection of peptide resins, the crude synthetic peptides were dissolved in aq. 30 % acetonitrile solution and separated by RP-HPLC on a semi-preparative C_{18} column (10 mm × 250 mm; Nacalai Tesque). They were further purified by cation-exchange chromatography and C_4 RP-HPLC as described above. The structural identity of synthetic and natural peptides was verified by co-elution experiments using capillary zone electrophoresis (CZE) and cation-exchange HPLC, and by MALDI–TOF-MS.

Capillary electrophoresis

CZE analyses were performed on a Jasco system (Jasco, Tokyo, Japan) equipped with a UV detector connected to a Shimadzu CR-4A recorder and a 70-cm capillary (0.1 μm internal diameter, 70 cm length, 50 cm to detector); 20 mM sodium citrate buffer, pH 2.5 (Applied Biosystems) was used for the analysis. Samples, dissolved in 20 mM sodium citrate, pH 2.5, were applied hydrodynamically to the capillary (height 20 cm, 15 s) and analyses were performed with a 20 kV constant voltage decrease. Effluent was monitored at 210 nm.

CD measurements

CD spectra were recorded on a J-725 spectropolarimeter (Jasco). The spectra were measured from 260 to 178 nm on samples in PBS, 60 % trifluoroethanol (TFE), pH 7.1, or PBS plus 120 mM dodecylphosphocholine (DPC), pH 7.2, at room temperature, with a 1-mm-path-length cell. Data were collected at 0.1 nm with a scan rate of 100 nm/min and a time constant of 0.5 s. The concentration of the toxins was 100 μg/ml. Data were the average of ten separate recordings and were analysed by the method of Bohm et al. [18] (also found at http://www.cryst.bbk.ac.uk/cdweb/html).

NMR structure determination

One- and two-dimensional ^{1}H NMR spectra were recorded on 500 and 600 MHz spectrometers (Bruker Analytik, Rheinstetten, Germany), essentially as described previously [19], but with water suppression by means of pulsed field gradients using the WATERGATE scheme and a 3-9-19 selective pulse [20]. These spectra were acquired on the following samples of synthetic pandinin 2: 2 mM in 90 % ^1H_2O/10 % ^2H_2O (v/v), pH 4.9, at 277 and 293 K; 2 mM in 60 % TFE (trifluoroethanol-$^2H_3$; Cambridge Isotope Laboratories, Ander, MA, U.S.A.)/40 % H_2O, pH 6.0, at 278, 283 (600 MHz) and 293 K (500 and 600 MHz); 3 mM in 120 mM DPC (dodecylphosphocholine-$^2H_{38}$; Cambridge Isotope Laboratories) micelles in 90 % ^1H_2O/10 % ^2H_2O (v/v), pH 5.4, at 298 and 308 K (600 MHz). Two series of one-dimensional spectra were acquired, one at increasing TFE levels from 0 to 60 % in water at 293 K and the other at increasing temperatures from 298 to 333 K on the sample in DPC. In addition, a ^{13}C heteronuclear multiple quantum coherence ('HMQC') spectrum [21] was recorded at 500 MHz and 308 K on the DPC sample, with 512 t_1 increments, 256 scans per increment, and a sweep width of 18865 Hz in the ^{13}C dimension. Chemical shifts were measured using various internal standards depending on the sample, and are referenced to 2,2-dimethyl-2-silapentane-5-sulphonate at 0 p.p.m.

Structure calculations

Methods for obtaining distance and angle restraints, generating structures in DYANA [22] and refining the structures by restrained simulated annealing and restrained energy minimization in X-PLOR [23], were as described previously [19] except that distances were calculated using CALIBA, where the volumes of backbone cross-peaks were proportional to r^{-6} and of cross-peaks involving side chains were proportional to r^{-4}. The final NMR restraint lists (from which distant restraints redundant with the covalent geometry had been eliminated by DYANA) were as follows: for pandinin 2 in 60 % TFE, 107 intra-residue, 64 sequential, 32 medium-range ($2 \leqslant |i–j| \leqslant 4$) and 0 long-range ($|i–j| \geqslant 5$) upper bound restraints, no lower bound restraints, and 18 backbone and 0 side-chain dihedral angle restraints; for pandinin 2 in DPC micelles, 68 intra-residue, 109 sequential, 146 medium-range ($|i–j| < 5$) and no long-range ($|i–j| \geqslant 5$) upper bound restraints, no lower bound restraints, and 20 backbone and no side-chain dihedral angle restraints. As no positive ϕ angles were observed, ϕ angles for all residues other than Gly and Pro were constrained to lie between −10 and −170°. Of the 50 CHARMM-minimized structures, the best 20 were chosen on the basis of their stereochemical energies (i.e. excluding the electrostatic term). Structures were analysed using Insight II (Molecular Simulations, San Diego, CA, U.S.A.) and MOLMOL [24]. Hydrogen bonds were identified in MOLMOL using a maximum C-N distance of 2.4 Å (where 1 Å = 0.1 nm) and a maximum angular deviation of 35° from linearity.

RESULTS

Purification and sequence analysis

Crude *P. imperator* venom was first submitted to RP-HPLC (Figure 1). Fractions (81 in total) were collected and assayed for antimicrobial activity against *E. coli* and *B. subtilis*. A total of

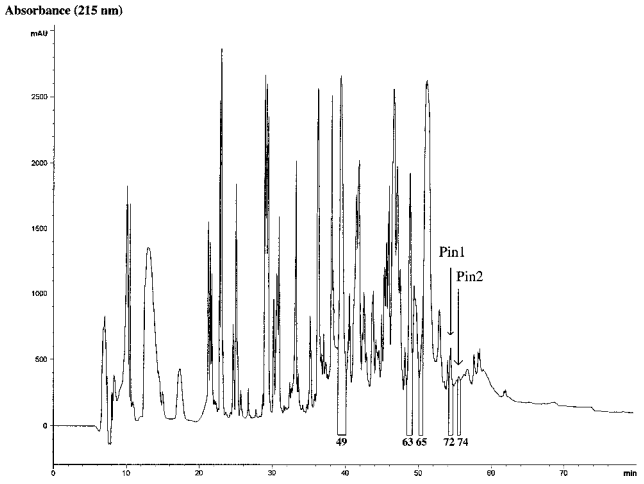

Figure 1 RP-HPLC chromatogram of crude *P. imperator* venom

The numbers (49, 63, 65, 72 and 74) represent HPLC fractions that gave positive results in the antimicrobial bioassays.

five fractions gave positive results in the bioassay. However, fractions 49, 63 and 65 induced an aggregation of the medium, preventing growth of the bacteria, so that it was not clear whether they had true antibiotic properties. Fraction 63, which corresponded to the antibacterial and antimalarial scorpine [15], slightly inhibited *E. coli* growth in our assay, whilst the highest antimicrobial activity was found in fractions 72 and 74. These two fractions were separated further by cation-exchange HPLC. Two single antimicrobial peptides were purified by a final RP-HPLC step and were obtained in pure form, as determined by CZE (results not shown), and named pandinin 1 (fraction 72) and pandinin 2 (fraction 74).

MALDI–TOF-MS analysis showed that the molecular masses of both peptides were not changed by reduction/alkylation, indicating that they did not contain cysteine residues paired to form disulphide bridges. Direct Edman degradation sequencing of pandinin 1 yielded the first 28 amino acid residues. Tryptic digestion yielded more than 6 peptides, which were sequenced to allow complete sequence determination (Figure 2A). Two endoproteinase Glu-C fragments were also sequenced and fully confirmed pandinin 1 sequence as a 44-residue basic peptide (calculated pI 10.28) with a carboxylated free C-terminus (Figure 2A). The average and monoisotopic molecular-mass values calculated from the sequence data (4799.55 and 4796.60 Da) were in excellent agreement with molecular-mass values measured in linear mode (average, 4799.20 Da) and reflector mode (monoisotopic, 4796.66 Da). Direct sequencing of pandinin 2 gave a peptide of 24 amino acid residues (Figure 2A). As the calculated average (2612.11 Da) and monoisotopic (2610.46 Da) molecular masses matched the measured values (average, 2612.60 Da; monoisotopic, 2610.46 Da), and sequencing data were clear, no further characterization steps were undertaken. Pandinin 2 is a basic peptide (calculated pI 10.52) with a carboxylated free C-terminal residue as suggested by MS data.

As other scorpion antimicrobial peptides have been found in the haemolymph, RP-HPLC fractions of *P. imperator* haemolymph were analysed by MALDI–TOF-MS to search for pandinin 1 and pandinin 2. No ions corresponding to their calculated molecular masses could be detected (results not shown). Therefore it appears that pandinin 1 and pandinin 2 are

A

```
Pandinin1   GKVWDWIKSAAKKIWSSEPVSQLKGQVLNAAKNYVAEKIGATPT
            <-------------------------->Direct
            <------><--><----------><------><-----><---->Trypsin
            <---------------><------------------------>Glu-C
Pandinin2   FWGALAKGALKLIPSLFSSFSKKD
            <---------------------->Direct
```

B

```
                                                                  % sim
Pandinin 1      GKVWDW-IKSAAKKIWSSEPVSQLKGQVLNAAKNYVAEKIGATPT-----   100
Hadrurin        G-ILDT-IKSIASKVWNSKTVQDLK----RKGINWVANKLGVSPQAA---   73.9
Adenoregulin    G-LWSK-IKEVGKE------AAKAA------AKAAGKAALGAVSEAV---   63.1
Cecropin A      --KWKL-FKKIEK-VGQNIRDGIIK-------AGPAVAVVGQATQIAK--   61.8
Gaegurin 4      G-ILDT-LKQFAKGVGKDLVKGAAQG-----VLSTVSCKLALTC------   58.8
Sarcotoxin IA   G-WLKK-IGKKIERVGQHTRDATIQG----LGIAQQAANVAATAR-----   58.3
Brevinin 2e     G-IMDT-LKNLAKTAG----KGALQS-----LLNKASCKLSGQC------   55.7
LycotoxinII     --KIKW-FKTMKS-------IAKFI------AKEQMKKHLGGE-------   52.7
Parabutoporin   ---FK-LGSFLKKAWKSKLAKKLRAKGKEMLKDYAKGLLEGGSEEVPGQ   48.6
```

C

```
                                                                  % sim
Pandinin 2      FWGALAKGALKLIPSLFSSFSKKD--                          100
Brevinin 1      FLPVLAGIAAKVVPALFCKITKKC--                          75.2
Gaegurin 5      FLGALFKVASKVLPSVKCAITKKC--                          73.2
Pipinin 1       FLPIIAGVAAKVFPKIFCAISKKC--                          72.2
Pipinin 3       FLPIIASVAAKVFSKIFCAISKKC--                          72.0
Pipinin 2       FLPIIAGIAAKVFPKIFCAISKKC--                          71.4
Gaegurin 6      FLPLLAGLAANFLPTIICKISYKC--                          67.0
Melittin        GIGAVLKVLTTGLPALISWIKRKRQQ                          63.4
Magainin 1      GIGKFLHSAGKFGKAFVGEIMKS---                          60.4
Magainin 2      GIGKFLHSAKKFGKAFVGEIMNS---                          59.7
```

D

```
                  10        20        30        40
                   |         |         |         |
Pandinin 1  GKVWDWIKSAAKKIWSSEPVSQLKGQVLNAAKNYVAEKIGATPT
Sec.Cons.   ccchhhhhhhhhhcccccchhhhhhhhhhhhhhhhhhhccccc
                   |         |         |         |
Pandinin 2  FWGALAKGALKLIPSLFSSFSKKD
Sec.Cons.   chhhhhhhhhhhhhhhhhc?cccc
```

Figure 2 Sequences of pandinins and multiple alignments

(**A**) Amino acid sequences of *P. imperator* antimicrobial toxins. (**B**) and (**C**) Sequence aligment of pandinins 1 and 2 with other amphipathic antimicrobial peptides. The sequences were aligned with Clustal W using a PAM 250 matrix. For clarity, the order of the sequences was modified after alignment. Percentage of sequence similarity relative to pandinin 1 and pandinin 2 is represented by % sim. Sequences are from the following references: hadrurin [16], adenoregulin [50], cecropin A [51], gaegurins [36], sarcotoxin IA [52], brevinin 2e [53], lycotoxins [9], parabutoporin [17], brevinin 1 [26], pipinins [37], magainins [25], melittin [54]. (**D**) Secondary structure prediction. Consensus structures were generated by the NPS@ server (c = coil, h = helix). Sec.Cons., Secondary structure consensus.

present only in the venom of *P. imperator*, in unchallenged scorpions at least.

Peptide synthesis

In order to confirm the structure of pandinin 1 and 2, and to further explore their biological properties, the two peptides were synthesized. In addition, the two C-terminal forms of pandinin 2 were synthesized and purified by RP-HPLC to determine whether amidation of the C-terminus affected antimicrobial activity. On the basis of a theoretical 0.15 mmol mass assembly for sPin1-OH, sPin2-OH and sPin-NH_2, the overall yields of the linear peptides after the first HPLC purification were estimated to be 12, 24 and 21 % respectively. The identity of synthetic pandinin 1 (sPin1-OH) and native pandinin 1 was confirmed by CZE co-elution and MS measurements of monoisotopic molecular masses (4796.64 and 4796.66 Da respectively), thus confirming a carboxylated C-terminus.

CZE co-elution experiments also demonstrated that native pandinin 2 co-eluted in a single peak with carboxylated sPin2-OH, but not with amidated sPin2-NH_2 (results not shown). The identity of sPin2-OH and native pandinin 2 was further confirmed by MS measurement of their monoisotopic molecular masses (2610.61 and 2610.46 Da respectively) and Edman sequencing of the synthetic peptide. The synthetic peptides were subsequently

Table 1 Antimicrobial activity of pandinin 1, pandinin 2 and magainin 1

	Minimal inhibitory concentration (μM)*		
Micro-organism	Pandinin 1	Pandinin 2	Magainin 1
Ps. aeruginosa	> 20.8	38.2	> 41.5
E. coli	20.8	19.1	> 41.5
Ent. faecalis	1.3	2.4	10.4
C. albicans	> 20.8	19.1	> 41.5
B. subtilis	5.2	4.8	41.5
Staph. epidermidis	5.2	4.8	20.8
Staph. aureus	2.6	2.4	20.8

* Data are the result of two independent trials.

Table 2 Haemolytic activity of pandinin 1, pandinin 2 and magainin 1

Results are the percentage of erythrocyte haemolysis and expressed as means ± S.D. of two independent trials.

Concentration (μM)	sPin1	sPin2	Magainin 1
44.5	1.4 ± 0.3	90.5 ± 0.8	2.4 ± 0.3
22.2	1.1 ± 0.3	51.4 ± 0.5	2.2 ± 1.1
11.1	0.9 ± 0.1	17.5 ± 1.1	1.8 ± 0.5
5.5	0.7 ± 0.3	3.7 ± 0.1	1.6 ± 0.3
2.7	0.2 ± 0.1	1.4 ± 0.3	1.2 ± 0.1

used in the structural determination and biological activity experiments.

Antimicrobial and haemolytic activity

The MIC values of various antimicrobial peptides obtained from the literature cannot be easily compared, as different strains of both micro-organisms and experimental conditions are used. The antimicrobial activities of pandinin 1 and pandinin 2 were assayed against the Gram-positive bacteria *B. subtilis*, *Staph. epidermidis*, *Ent. faecalis* and *Staph. aureus*, the Gram-negative *Ps. aeruginosa* and *E. coli* and the yeast *C. albicans*, and compared with that of magainin 1, a potent bactericide from the skin of the frog *Xenopus laevis* [25].

Under our bioassay conditions, the pandinins displayed potent activity, with a degree of variation between the target micro-organisms. Both peptides appeared to have approximately the same spectrum of activity as magainin 1, within the scope of this study (Table 1). Pandinin 1 and pandinin 2 had weak activity against two of the Gram-negative bacteria tested, but showed higher activity against the strains of Gram-positive bacteria tested, with pandinin 2 being generally more active than magainin 1. Indeed, in our bioassay, pandinin 2 was almost 10 times more active against *B. subtilis* and *Staph. aureus* than magainin 1. *C. albicans* was resistant to the peptides, although pandinin 2 demonstrated some activity with an MIC of 19.1 μM. Both sPin2-OH and sPin2-NH_2 were equally toxic to *E. coli* and *B. subtilis*, suggesting that C-terminal amidation has no effect on the activity spectrum of pandinin 2. Results obtained with magainin 1 in our bioassays were consistent with previous findings [25–27].

Haemolytic assays of magainin 1 and pandinin 2 on sheep erythrocytes showed that pandinin 2 had higher haemolytic activity than magainin 1, with 51% haemolysis observed at 22.2 μM for pandinin 2, but only 2% for magainin 1 at a similar concentration (Table 2). The two C-terminal forms of sPin2 were equally haemolytic (results not shown). In contrast, pandinin 1 induced only 1.4% haemolysis at the highest concentration used in the assay and displayed even weaker haemolytic activity than magainin 1.

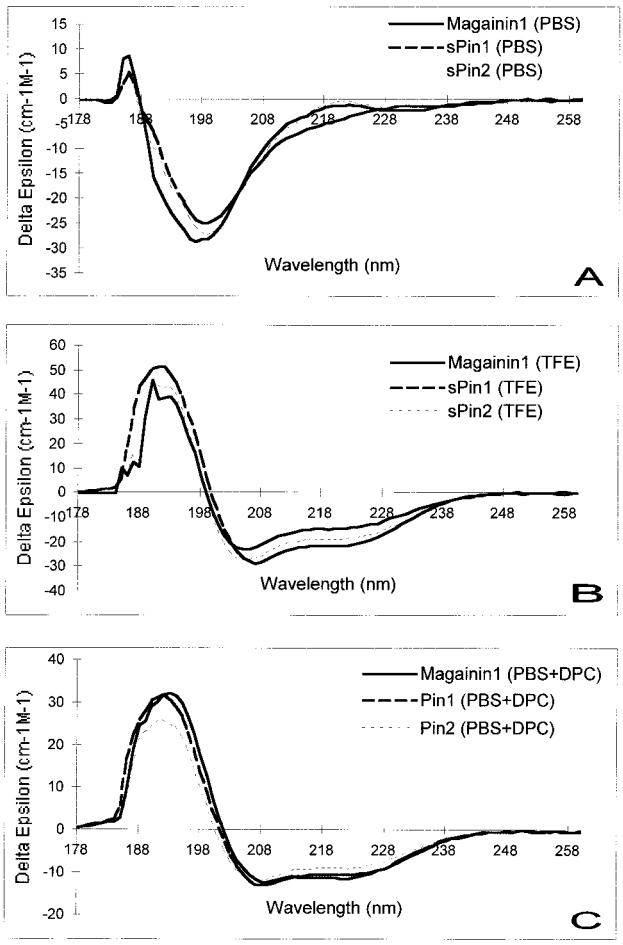

Figure 3 CD spectra

Spectra of synthetic pandinin 1, synthetic pandinin 2 and magainin 1 in (**A**) PBS, (**B**) 60% TFE and (**C**) PBS plus 120 mM DPC, pH 7.2.

CD measurements and structure prediction

The secondary structure analysis was performed using CD spectral data from 178 to 260 nm and the spectra of sPin1-OH and sPin2-OH compared with that of magainin 1 (Figure 3). Magainin 1 and both pandinins showed an unordered structure in aqueous solution, characterized by a strong minimum around 200 nm and a weaker one at approx. 220 nm (Figure 3A). In the presence of 60% TFE or in the presence of 120 mM DPC, the CD spectra of both peptides changed dramatically and indicated a more ordered structure, with a maximum ellipticity at 190–195 nm and a decrease of the signal at 208 and 222 nm (Figures 3B and 3C). These data are consistent with the formation of an α-helix in aqueous TFE or in a DPC membrane-mimetic environment, as previously observed with other amphipathic antimicrobial peptides [28–30]. The CD spectra of sPin2-OH and sPin2-NH_2 were essentially identical (results not shown). The CD spectra of magainin 1 and pandinins in 120 mM DPC were comparable in their interpreted secondary structure components,

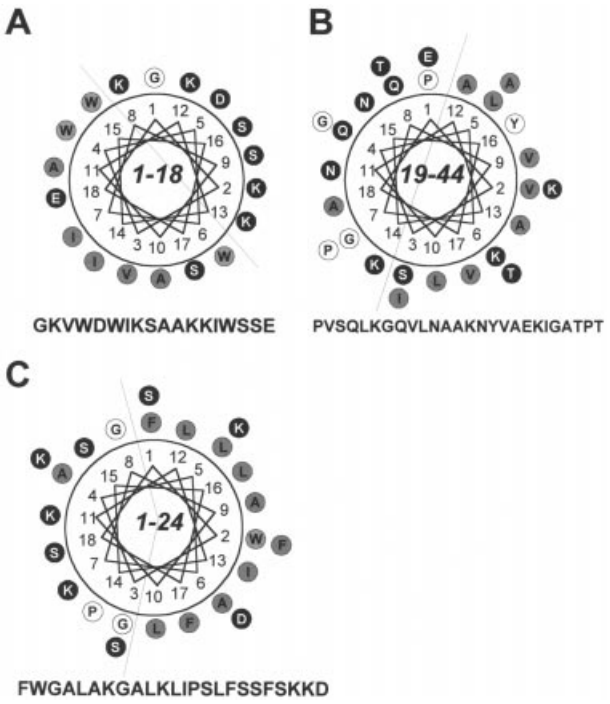

Figure 4 Helical-wheel projections of pandinins

(**A**) and (**B**) Pandinin 1 and (**C**) Pandinin 2. In the case of pandinin 1 the two predicted helical regions 1–18 (**A**) and 19–44 (**B**) (see Figure 2) are shown separately. Charged residues are shown in black, hydrophobic residues are shown in grey and neutral residues in white. The dotted lines represent the division between the hydrophilic side and the hydrophobic side of the amphipathic residues.

with α-helical contents of 96.0, 96.4 and 95.3 % for magainin 1, sPin1-OH and sPin2-OH respectively. Values for antiparallel β-sheet (0.0, 0.0 and 0.0 %), parallel β-sheet (0.5, 0.5 and 0.6 %), β-turns (6.3, 5.9 and 6.7 %), and random coil (1.3, 1.5 and 1.3 %) were very low.

The secondary structure prediction of pandinin 2 obtained from the NPSA server (http://pbil.ibcp.fr/NPSA) showed an α-helical conformation for residues 2–18 (Figure 2D). For pandinin 1, two α-helical regions were predicted (residues 3–14 and 20–39), separated by a random coil region including Pro[19] (WSSEP). Structures involving two helices separated by a flexible hinge region or a kink in the chain associated with a proline have been reported for melittin [31], caerin 1.1 [29], sarcotoxin IA [32] or cecropin A [33]. Pandinin 1 shows an extensive coil region, which could allow significant flexibility in the inter-helical region. A helical-wheel diagram (Figure 4C) shows that the helix is markedly amphipathic, with a significant non-polar surface.

The antimicrobial activities of pandinins 1 and 2 were similar, but only pandinin 2 possessed strong haemolytic activity. As their helical contents inferred from CD data were similar (99.3 and 99.0 % respectively), we decided to determine a high-resolution structure for pandinin 2 in solution using NMR spectroscopy.

NMR structure of pandinin 2

Initial ^{1}H NMR spectra of pandinin 2 in water showed little spectral dispersion, consistent with a lack of ordered structure. Addition of the helix-stabilizing co-solvent TFE [34] increased the spectral dispersion, most notably in the backbone amide region, confirming that pandinin 2 adopts a helical structure in the presence of TFE. Spectra at 40 and 50 % TFE were rather broad, whereas spectra at 60 % TFE were quite sharp and well-dispersed, thus this solvent was used to record two-dimensional spectra for resonance assignments and structure determination.

Detergent micelles also represent a useful milieu for high-resolution NMR studies of the structures of peptides and proteins in a membrane-mimetic environment [30]. As our structure calculations on pandinin 2 in 60 % TFE in water indicated that

Table 3 Structural statistics for the 20 energy-minimized structures of pandinin 2 in DPC micelles from X-PLOR

The best 20 structures after energy minimization in the distance geometry force field of X-PLOR were subsequently energy minimized in the CHARMM force field, using a distance-dependent dielectric. Values represent means ± S.D. Abbreviations: E_{NOE}, nuclear Overhauser effect distance restraints energy; E_{cdih}, dihedral angle restraints energy; $E_{L\text{-}J}$, Lennard-Jones energy; E_{elec}, intramolecular electrostatic energy; RMSD, root mean square deviation.

(a)

Parameter	Value
RMS deviations from experimental distance restraints (Å) (313)*	0.015 ± 0.001
RMS deviations from experimental dihedral restraints (°) (20)*	0.18 ± 0.06
RMS deviations from idealized geometry:	
Bonds (Å)	0.0092 ± 0.0005
Angles (°)	2.26 ± 0.05
Impropers (°)	0.27 ± 0.02
Energies (kcal · mol^{-1})	
E_{NOE}	3.6 ± 0.4
E_{cdih}	0.05 ± 0.03
$E_{L\text{-}J}$	−73 ± 4
$E_{bond} + E_{angle} + E_{improper}$	55 ± 3
E_{elec}	−259 ± 17

(b)

	Mean pairwise RMSD (Å)	
Residues	Backbone heavy atoms	All heavy atoms
1–24	1.72 ± 0.44	2.78 ± 0.57
1–20	0.98 ± 0.28	1.49 ± 0.32

* The numbers of restraints are shown in parentheses. None of the structures had distance violations > 0.3 or dihedral angle violations > 5°.

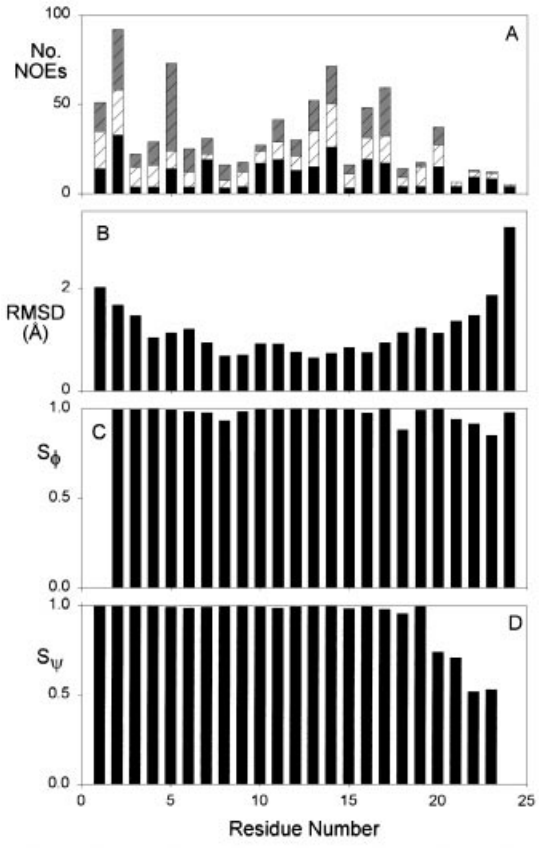

Figure 5 Parameters characterizing the final 20 structures of pandinin 2 in DPC micelles at 308 K, plotted as a function of residue number

(**A**) Upper-bound restraints used in final round of structural refinement shown as medium-range (grey), sequential (diagonal shading) and intra-residue (black). NOE, nuclear Overhauser effect. (**B**) RMS differences from mean structure for N, C^{α} and C atoms following superposition over the whole molecule. (**C**) and (**D**) Angular order parameters (S) for the backbone dihedral angles ϕ and ψ.

it was predominantly helical, and the functional data indicate that it acts on biological membranes, we have also determined its structure in DPC micelles. The peptide dissolved readily in this solution and gave high-quality NMR spectra. The structural statistics for pandinin 2 in DPC micelles (Table 3) show that the structures are in good agreement with the experimental restraints (Figure 5A) and have good stereochemistry. Moreover, 100 % of the residues have ϕ–ψ values in the generously allowed regions of a Ramachandran plot. The angular order parameters (S) of the final 20 structures indicate that residues 1–20 are well defined locally, with $S > 0.8$ for both ϕ and ψ angles (Figures 5C and 5D). The backbone root mean square deviation (RMSD) from the mean structure (Figure 5B) also shows that the structure is well defined over most of the molecule. Mean pairwise RMS differences calculated over the backbone heavy atoms (N, C^{a} and C) and all heavy atoms respectively of the whole molecule were 1.72 ± 0.44 and 2.78 ± 0.57 Å, and for the well-defined region 0.98 ± 0.28 and 1.49 ± 0.32 Å. On the basis of backbone dihedral angles and hydrogen-bonding patterns, pandinin 2 is helical in DPC micelles up to residues 18–19, with no significant kink around the proline at position 14. This result is in good agreement with the predicted structure described above. Figure 6 shows stereo views of the best 20 structures (Figure 6A) and a ribbon diagram of the closest-to-average structure (Figure 6B).

Temperature dependence

One-dimensional ^{1}H NMR spectra of pandinin 2 in DPC micelles showed significant upfield shifts for the Phe^1 aromatic resonances from their random-coil values of around 7.3 p.p.m. [35]. These peaks and those of the adjacent Trp^2 aromatic side chain, were also broader than expected, although they sharpen up at elevated temperatures, as shown in Figure 7. This suggested that the N-terminal region of pandinin 2 was immobilized more than the C-terminus when bound to DPC micelles. The upfield shifts of the Phe^1, and to a lesser extent the Trp-2, aromatic resonances are consistent with ring-current interactions between these two side chains as illustrated in Figure 6(B). Additional structural data are available at http:/www.BiochemJ.org/bj/359/bj3590035add.htm which contains three Tables and one Figure.

DISCUSSION

Purification and characterization of andinins

Two novel peptides with inhibitory activity towards Gram-positive and Gram-negative bacteria were isolated from the venom of the scorpion *P. imperator* using bioassay-guided fractionation. The two antimicrobial peptides, pandinin 1 and pandinin 2, were eluted by a high percentage of acetonitrile from the RP-HPLC column, indicating a very hydrophobic character. Pandinin 2 is more hydrophobic than pandinin 1, and this characteristic may be related to differences in their activity, as discussed below. Overall peptide hydrophobicity and amphipathicity have been recognized as crucial determinants in defining the potency of cytotoxic and antimicrobial peptides, as they affect their ability to interact with various membrane phospholipids. Both the low abundance and the highly hydrophobic character of these peptides may explain why their presence has been overlooked in scorpion venoms. Classical extraction methods predominantly use acidified water or weak acid solutions and thus will not properly extract such peptides. Indeed, in our hands, another *P. imperator* venom sample extracted with water/0.1 % TFA only, did not show the presence of pandinins, which were most likely excluded from the extraction process. Indeed, a previous study using *P. imperator* failed to report antimicrobial activity for this venom [16].

Pandinins appear to be integral components of scorpion venom as they were not detected in haemolymph, although their circulating levels could be extremely low in unchallenged scorpions. This result provides additional evidence for a significant role of α-helical amphipathic antimicrobial peptides in venoms of scorpions, either as components of the immune system of these animals or as synergistic cofactors for toxins, as they have been shown to dissipate ion gradients across membranes [9,17]. Our work complements the recent discovery of structurally related peptides in other scorpion venoms [16,17]. Previous findings have demonstrated the presence of β-sheet-containing disulphide-rich antimicrobial peptides in scorpion haemolymph, analogous to the well-studied production of defensins by insects.

Pandinins 1 and 2 belong to a large group of α-helical antimicrobial peptides. Their primary structures are typically those of cationic amphipathic peptides, with alternating cationic and hydrophobic residues. A sequence database search for pandinin 1 did not reveal a high homology with any other antimicrobial peptides. The highest degree of similarity was observed with hadrurin (73.9 %), another scorpion venom antimicrobial peptide recently discovered [16]. Pandinin 1 also has limited homology with adenoregulin, brevinin 2e and gaegurin 4

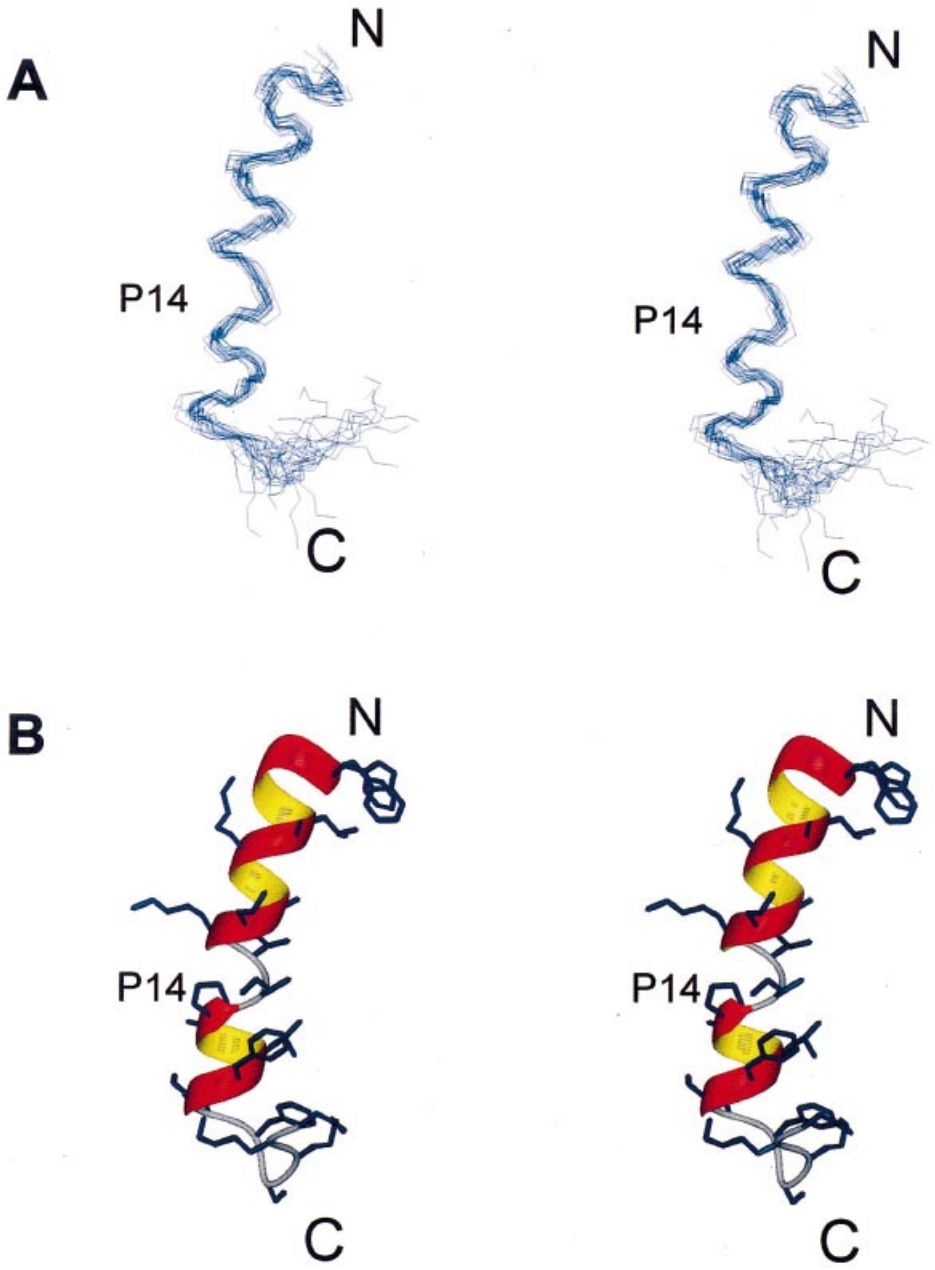

Figure 6 Solution structure of pandinin 2 in DPC micelles

(**A**) Stereo view of the backbone heavy atoms (N, C^{α} and C) of the final 20 structures, superimposed over the backbone heavy atoms of residues 1–20. Generated using Insight II. (**B**) Stereo view of the structure closest to the average over the family of 20, with all atoms shown. The backbone is highlighted with a ribbon, the side chains are shown in thick lines and the molecule is oriented as (**A**). Generated using MOLMOL.

from frog skin, sarcotoxin IA and cecropin A (55–63 %). The lowest homology (48–52 %) among the sequences compared was observed for lycotoxin II and parabutoporin, other peptides from arachnid venoms, demonstrating the high degree of sequence diversification of this class of peptides in arachnid venoms (Figure 2B).

Pandinin 2 belongs to the group of shorter α-helical magainin-type peptides and shows significant homology with several frog antimicrobial peptides (Figure 2C): brevinin 1 from *Rana brevipoda porsa* [26], gaegurins 5 and 6 from the skin of *Rana rugosa* [36], the pipinins from *Rana pipiens* [37] and the magainins from *Xenopus laevis* [25]. No other arachnid antimicrobial peptide isolated to date has significant similarity to pandinin 2, and it is the first representative of this subclass of antimicrobial peptides to be isolated from an arachnid.

The high degree of homology between *P. imperator* peptides and frog skin peptides is interesting and may suggest high phylogenetic conservation of these structure based upon early selection pressure. Additionally, it may indicate that these peptides have been conserved in the evolutionary process due to their activity against a broad range of pathogenic micro-organisms.

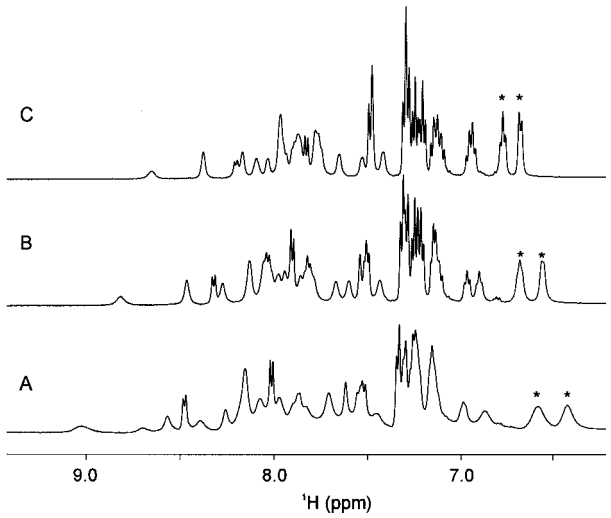

Figure 7 Temperature-dependence of one-dimensional ^{1}H NMR spectra of pandinin 2 in DPC micelles

(**A**) 298 K. (**B**) 317 K. (**C**) 333 K. Spectra were recorded at 500 MHz. Two aromatic resonances from Phe[1] that show significant temperature dependence are labelled with asterisks.

Biological activity of pandinins

Our results clearly support the classification of pandinins as antimicrobial peptides, possessing pore-forming activity. The activity of both pandinins is at the lower extremity of the activity range described for this kind of peptide (MIC 1.3–38.2 μM, compared with the most active peptides at $< 10\,\mu$M). Both biological assays and structural data imply that pandinins may act by a molecular mechanism similar to that of melittin or the magainins. The peptides adopt a well-defined α-helical amphipathic structure when in contact with 60 % TFE or cell membrane phospholipids, as demonstrated by CD and NMR data. Interaction with the phospholipids undoubtedly results in membrane disruption and cell lysis, as illustrated by the activity observed against bacteria in our bioassays. The observed antimicrobial activity of pandinins correlates well with previous reports indicating that Gram-positive bacteria may be less resistant to cytolytic antimicrobials, whilst Gram-negative and fungi are more resistant [9,25,29,36]. In addition, pandinin 2 causes haemolysis of sheep erythrocytes in less than 60 min, demonstrating its ability to interact not only with charged phospholipids, but also with zwitterionic membranes. Its ability to lyse eukaryotic cells is similar to that of other α-helical cationic peptides from venoms such as hadrurin [16] and melittin [38], and may have a role in venom toxicity by dissipating ion gradients, affecting membrane potential and thus acting in a synergistic manner with ion-channel toxins. Pandinin 1 has no haemolytic activity and thus may act in a similar manner to magainin 1, as a specific antimicrobial component in the venom. Both pandinins have pI values > 10, which indicates that they will remain positively charged at neutral pH and will thus strongly interact with negatively charged membrane phospholipids.

In the group structurally related to pandinin 2, lycotoxins are also more haemolytic than magainins [9]. However, gaegurins do not induce haemolysis of human erythrocytes even at concentrations up to 38 μM, while pandinin 2 produces around 90 % haemolysis of sheep erythrocytes at a similar concentration. The cytolytic activity of magainin-like peptides appear to depend on the lipid composition and charge of the cell membranes, so that permeabilization is achieved via different mechanisms, for instance a 'carpet-like' effect [39] or formation of a 'toroidal' pore [40]. However, it has been noted that peptides having both haemolytic and antimicrobial activity were more effective in permeabilizing lipid vesicles when compared with peptides having only antibacterial or low haemolytic activity [41]. The ability to interact more strongly with membranes of various charges may thus be a selective advantage for venom antimicrobial peptides, giving them a broad spectrum of activity and the possibility of disrupting cell membranes to enhance the action of other venom components.

Amphipathic peptides having either carboxylated or amidated C-terminals were previously reported from the skin of *Rana* sp. frogs [42] and the venom of *Lycosa caroliniensis* [9]. Although the introduction of an amide group could have an impact on overall peptide charge and therefore interaction with membrane phospholipids and permeabilization properties, no such effect was detected in our bioassays using the two sPin2 C-terminal forms. This may be explained by the fact that initial membrane insertion proceeds from the N-terminal peptide end and that further interaction of the C-terminal end may be less crucial in modulating overall activity.

Structure of pandinins

Although the three-dimensional structure of pandinin 1 in DPC micelles was not determined experimentally, secondary-structure prediction algorithms suggest that pandinin 1 is likely to consist of two distinct amphipathic α-helices separated by an unstructured hinge region incorporating the Pro[19] residue. Similar structures have been reported for cecropin A, where the unstructured region is centred on Pro[23] [33], cecropin B1, where Gly[23], Pro[24] and Lys[25] form a hinge between helices encompassing residues 3–22 and 26–33 [43], and sarcotoxin 1A, where the four residues Gly[24]–Ile[27] constitute the hinge region [32], although in that case the hinge region is characterized by glycine residues, which are known to be helix breakers. It may thus be hypothesized that the structure of pandinin 1 in phospholipid micelles, or in contact with membrane phospholipids, will resemble that of cecropin A, cecropin B1 and sarcotoxin 1A. An Edmundson helical wheel projection indicates that pandinin 1 has a marked amphipathic character, with basic and hydrophobic residues evenly distributed on opposite sides of the α-helix. Of its seven lysine residues, six are found on the same side of the molecule (Figures 4A and 4B). Previous studies have demonstrated that modification of the hinge region induces significant changes in peptide activity [29], most likely by affecting the angle formed by the two helices, thus modifying their amphipathic orientation and their ability to interact with membranes. The arrangement of long antimicrobial α-helical peptides into two separate helices joined by a flexible region appears to be a common feature and could possibly play a crucial role in their specificity against the variously charged biological membranes resulting from the association of many different phospholipids.

Pandinin 2 clearly forms a helical structure in the presence of DPC micelles (Figure 3C). Inspection of a helical wheel diagram of this structure (Figure 4C) shows that it is markedly amphipathic, with a large non-polar surface and all Lys residues except one located on the other side. As a corollary, the N-terminus and lysine residues at positions 7 and 11 form a significant positively charged surface on one face of the peptide, and no doubt contribute to its interaction with the charged phosphocholine head groups of DPC. It is likely that pandinin 2 lies on the surface of the DPC micelles, with the apolar surface at least

partially buried in the lipid and the positively charged groups at the surface in the vicinity of the DPC head groups. Our NMR data also suggest that the N-terminal region is less mobile than the C-terminus, no doubt reflecting its lower polarity and more stable helical structure. This suggests that the N-terminus of pandinin 2 is more deeply buried in the lipid phase than the C-terminus. The presence of a significant positively charged surface implies that pandinin 2 is likely to interact more strongly with negatively charged membranes than with zwitterionic or neutral membranes. However, recent studies on a designed amphipathic peptide antibiotic LAH_4 [44] suggest that, although the interaction with negatively charged membranes might be stronger, the lytic activity against these membranes may not be, perhaps because of stabilization of a 'pre-lytic' state of the peptide. Results obtained with pandinin 2 appear to support the latter, since pandinin 2 is clearly haemolytic and not only antimicrobial.

To date, no satisfactory structure–activity relationship has been proposed to explain the differential activity of the antimicrobial peptides on bacterial and erythrocyte membranes, and several physical parameters are thought to be involved [45]. Preferred interaction with either membrane type may result from a complex combination of factors such as hydrophobicity, amphipathic character, and overall peptide charge. Changes in haemolytic and membrane permeabilizing efficiency have been tentatively linked to a subtle balance between polar and hydrophobic domains measured by the angle formed by both domains respective to the axis of the helix. Haemolytic activity of the magainins was enhanced by an increase in the polar domain [45], and antimicrobial activity has been correlated to an increase in positive charges which is thought to enhance association with negatively charged phospholipids. Melittin, which is both antimicrobial and haemolytic, has a distinctly hydrophobic N-terminus and a charged C-terminus, whereas magainin, which has no haemolytic activity, lacks the hydrophobic N-terminus and, similar to pandinin 1, has an overall homogeneous distribution of hydrophobic and hydrophilic residues. In contrast, pandinin 2 has a distribution of charges resembling that of melittin, and also demonstrates both types of activity.

One of the key structural features for membrane selectivity could be the amphipathic nature of the peptide N-terminal region as demonstrated in a recent study on a diastereoisomer of melittin [46]. While the N-terminal amphipathic helical structure is not required for the cytolytic activity toward negatively charged membranes and bacterial cells, it appears to be a crucial structural element for binding and insertion into zwitterionic membranes and for haemolytic activity. In this respect, pandinin 2 is an interesting model which could be used similarly to melittin to elucidate the biophysical features controlling membrane selectivity in short magainin-type peptides.

The relevance of the structure we observe in lipid micelles with respect to the lytic activity of pandinin 2 in biological membranes, is that it probably represents the form of the peptide that initially contacts the membrane and then begins to insert into the lipid. If cell lysis was due to pore formation, the helix would be expected to subsequently orient itself normal to the plane of the bilayer, although this entails an energetic penalty associated with moving the positively charged groups into the membrane [47]. However, recent results lend support to a detergent-like action of amphipathic helical peptides as the main cause of lytic activity rather than pore formation, thus obviating the need for transmembrane movement of the (positively charged) peptide [48]. The findings of Vogt and Bechinger [44] on the designed 26-residue peptide LAH_4 are of particular note in this context. At $pH < 6$, where its four histidine residues are protonated, LAH_4 is oriented parallel to the membrane surface, while at $pH > 7$ it assumes a transmembrane orientation. Nevertheless, its antibiotic activity is two orders of magnitude higher at acidic pH than at pH 7.5.

The absence of a marked kink in the helix of pandinin 2 around Pro^{14} distinguishes it from melittin, where the corresponding proline residue produces an angle of 126–160° (depending on the environment) between the N- and C-terminal helices. Replacement of Pro^{14} in melittin by alanine removed this bend but did not inactivate the molecule, even though its properties and spectrum of activity were altered [49]. The frog skin peptide magainin does not contain a proline residue, and as a result adopts an essentially linear helical structure with no kink [30]. Structurally, therefore, pandinin 2 resembles magainin more than melittin, although the overall sequence similarity is approximately the same (approx. 60 %). In addition, melittin is distinctly longer (28 residues) than the other peptides of this group (19–24 residues) (Figure 2).

The discovery of polycationic antimicrobial peptides in scorpion venom brings new insights into the mode of action of venom and also opens new avenues for the discovery of novel antibiotic molecules from arthropod venoms. Because of their strong antimicrobial activity, scorpion venom antimicrobial peptides have an interesting potential in applications for the therapeutic control of pathogenic bacteria. In this respect, haemolytic activity is clearly not a desirable feature in therapeutic peptides, and a comparison of the solution structures of pandinin 1 and hadrurin would be quite informative in identifying structural features responsible for haemolytic activity in the longest α-helical antimicrobial peptides. The latter lacks the central proline residue and is missing four residues, which could correspond to one turn of the helix predicted at that position. It would be interesting to establish whether these sequence differences translate to the expected structural differences and if, in turn, they are responsible for the absence of haemolytic activity in pandinin 1. This could be the object of further structural work involving selective mutagenesis of pandinin 1 and hadrurin, and the production of chimaeras as a way of defining the structural features of pandinin 1 that inactivate its haemolytic activity.

We are grateful to D. Saldanha for assistance with spectral analysis, to M. Hisada for help with MS measurements and to Dr H. Naoki for help in acquiring CD spectra.

REFERENCES

1 Larrick, J. W. and Wright, S. C. (1996) Cationic antimicrobial peptides. Drugs Future **21**, 41–48
2 Hancock, R. E. and Lehrer, R. (1998) Cationic peptides: a new source of antibiotics. Trends Biotechnol. **16**, 82–88
3 Csordas, A. and Michl, H. (1969) Primary structure of two oligopeptides of the toxin of *Bombina variegata*. Toxicon **7**, 103–108
4 Nicolas, P. and Mor, A. (1995) Peptides as weapons against microorganisms in the chemical defense system of vertebrates. Annu. Rev. Microbiol. **49**, 277–304
5 Bulet, P., Hetru, C., Dimarcq, J. L. and Hoffmann, D. (1999) Antimicrobial peptides in insects: structure and function. Dev. Comp. Immunol. **23**, 329–344
6 Hoffmann, J. A., Kafatos, F. C., Janeway, C. A. and Ezekowitz, R. A. (1999) Phylogenetic perspectives in innate immunity. Science (Washington, D.C.) **284**, 1313–1318
7 Hwang, P. M. and Vogel, H. J. (1998) Structure-function relationships of antimicrobial peptides. Biochem. Cell Biol. **76**, 235–246
8 Iwanaga, S., Kawabata, S. and Muta, T. (1998) New types of clotting factors and defense molecules found in horseshoe crab hemolymph: their structures and functions. J. Biochem. (Tokyo) **123**, 1–15
9 Yan, L. and Adams, M. E. (1998) Lycotoxins, antimicrobial peptides from venom of the wolf spider *Lycosa carolinensis*. J. Biol. Chem. **273**, 2059–2066
10 Xu, K., Ji, Y. and Qu, X. (1989) Purification and characterisation of an antibacterial peptide from venom of *Lycosa singoriensis*. Acta Zool. Sinica **35**, 300–305
11 Haeberli, S., Kuhn-Nentwig, L., Schaller, J. and Nentwig, W. (2000) Characterisation of antibacterial activity of peptides isolated from the venom of the spider *Cupiennius salei* (Araneae: Ctenidae). Toxicon **38**, 373–380

12 Silva, Jr, P. I., Daffre, S. and Bulet, P. (2000) Isolation and characterization of gomesin, an 18-residue cysteine-rich defense peptide from the spider *Acanthoscurria gomesiana* hemocytes with sequence similarities to horseshoe crab antimicrobial peptides of the tachyplesin family. J. Biol. Chem. **275**, 33464–33470

13 Cociancich, S., Goyffon, M., Bontems, F., Bulet, P., Bouet, F., Menez, A. and Hoffmann, J. (1993) Purification and characterization of a scorpion defensin, a 4 kDa antibacterial peptide presenting structural similarities with insect defensins and scorpion toxins. Biochem. Biophys. Res. Commun. **194**, 17–22

14 Ehret-Sabatier, L., Loew, D., Goyffon, M., Fehlbaum, P., Hoffmann, J. A., van Dorsselaer, A. and Bulet, P. (1996) Characterization of novel cysteine-rich antimicrobial peptides from scorpion blood. J. Biol. Chem. **271**, 29537–29544

15 Conde, R., Zamudio, F. Z., Rodriguez, M. H. and Possani, L. D. (2000) Scorpine, an anti-malaria and anti-bacterial agent purified from scorpion venom. FEBS Lett. **471**, 165–168

16 Torres-Larios, A., Gurrola, G. B., Zamudio, F. Z. and Possani, L. D. (2000) Hadrurin, a new antimicrobial peptide from the venom of the scorpion *Hadrurus aztecus*. Eur. J. Biochem. **267**, 5023–5031

17 Verdonck, F., Bosteels, S., Desmet, J., Moerman, L., Noppe, W., Willems, J., Tytgat, J. and Van der Walt, J. (2000) A novel class of pore-forming peptides in the venom of *Parabuthus schlechteri* Purcell (Scorpions: Buthidae). Cimbebasia **16**, 247–260

18 Bohm, G., Muhr, R. and Jaenicke, R. (1992) Quantitative analysis of protein far UV circular dichroism spectra by neural networks. Protein Eng. **5**, 191–195

19 Pallaghy, P. K., Alewood, D., Alewood, P. F. and Norton, R. S. (1997) Solution structure of robustoxin, the lethal neurotoxin from the funnel-web spider *Atrax robustus*. FEBS Lett. **419**, 191–196

20 Sklenar, V., Piotto, M., Leppik, R. and Saudek, V. (1993) Gradient-tailored water suppression for ^{1}H-^{15}N HSQC experiments optimized to retain full sensitivity. J. Magn. Reson. Ser. A **102**, 241–245

21 Bax, A., Griffey, R. H. and Hawkins, B. L. (1983) Correlation of proton and nitrogen-15 chemical shifts by multiple quantum NMR. J. Magn. Reson. **55**, 301–315

22 Güntert, P., Mumenthaler, C. and Wuthrich, K. (1997) Torsion angle dynamics for NMR structure calculation with the new program DYANA. J. Mol. Biol. **273**, 283–298

23 Brünger, A. T. (1992) X-PLOR Version 3.1. A System for X-ray Crystallography and NMR, Yale University, New Haven, CT

24 Koradi, R., Billeter, M. and Wüthrich, K. (1996) MOLMOL: A program for display and analysis of macromolecular structures. J. Mol. Graphics **14**, 51–55

25 Zasloff, M. (1987) Magainins, a class of antimicrobial peptides from *Xenopus* skin: isolation, characterization of two active forms, and partial cDNA sequence of a precursor. Proc. Natl. Acad. Sci. U.S.A. **84**, 5449–5453

26 Morikawa, N., Hagiwara, K. and Nakajima, T. (1992) Brevinin-1 and -2, unique antimicrobial peptides from the skin of the frog, *Rana brevipoda porsa*. Biochem. Biophys. Res. Commun. **189**, 184–190

27 Lee, K. Y., Hong, S. Y., Oh, J. E., Lee, B. J. and Choi, B. S. (1998) Antimicrobial activity and conformation of Gaegurin-6 amide and its analogs. Peptides **19**, 1653–1658

28 Batista, C. V. F., Rosendo da Silva, L., Sebben, A., Scaloni, A., Ferrara, L., Paiva, G. R., Olamendi-Portugal, T., Possani, L. D. and Bloch, J. C. (1999) Antimicrobial peptides from the Brazilian frog *Phyllomedusa distincta*. Peptides **20**, 679–686

29 Wong, H., Bowie, J. H. and Carver, J. A. (1997) The solution structure and activity of caerin 1.1, an antimicrobial peptide from the Australian green tree frog, *Litoria splendida*. Eur. J. Biochem. **247**, 545–557

30 Gesell, J., Zasloff, M. and Opella, S. J. (1997) Two-dimensional ^{1}H NMR experiments show that the 23-residue magainin antibiotic peptide is an alpha-helix in dodecylphosphocholine micelles, sodium dodecylsulfate, and trifluoroethanol/water solution. J. Biomol. NMR **9**, 127–135

31 Bazzo, R., Tappin, M. J., Pastore, A., Harvey, T. S., Carver, J. A. and Campbell, I. D. (1988) The structure of melittin. A ^{1}H-NMR study in methanol. Eur. J. Biochem. **173**, 139–46

32 Iwai, H., Nakajima, Y., Natori, S., Arata, Y. and Shimada, I. (1993) Solution conformation of an antibacterial peptide, sarcotoxin IA, as determined by ^{1}H-NMR. Eur. J. Biochem. **217**, 639–644

33 Holak, T. A., Engstrom, A., Kraulis, P. J., Lindeberg, G., Bennich, H., Jones, T. A., Gronenborn, A. M. and Clore, G. M. (1988) The solution conformation of the antibacterial peptide cecropin A: a nuclear magnetic resonance and dynamical simulated annealing study. Biochemistry **27**, 7620–7629

34 Sönnichsen, F. D., Van Eyk, J. E., Hodges, R. S. and Sykes, B. D. (1992) Effect of trifluoroethanol on protein secondary structure: an NMR and CD study using a synthetic actin peptide. Biochemistry **31**, 8790–8798

35 Wishart, D. S., Bigam, C. G., Holm, A., Hodges, R. S. and Sykes, B. D. (1995) ^{1}H, ^{13}C and ^{15}N random coil NMR chemical shifts of the common amino acids. I. Investigations of nearest-neighbor effects. J. Biomol. NMR **5**, 67–81

36 Park, J. M., Jung, J. E. and Lee, B. J. (1994) Antimicrobial peptides from the skin of a Korean frog, *Rana rugosa*. Biochem. Biophys. Res. Commun. **205**, 948–954

37 Pisano, J. J., Horikawa, R. and Argiolas, A. (1985) New lytic peptides in insect venoms and frog skin. 9th American Peptide Symposium, Toronto, Canada

38 Fennell, J. F., Shipman, W. H. and Cole, L. J. (1968) Antibacterial action of melittin, a polypeptide from bee venom. Proc. Soc. Exp. Biol. Med. **127**, 707–710

39 Shai, Y. (1995) Molecular recognition between membrane-spanning polypeptides. Trends Biochem. Sci. **20**, 460–464

40 Ludtke, S., He, K., Heller, W. T., Harroun, T. A., Yang, L. and Huang, H. W. (1996) Membrane pores induced by magainin. Biochemistry **35**, 13723–13728

41 Sitaram, N. and Ramakrishnan, N. (1999) Interaction of antimicrobial peptides with biological and model membranes: structural and charge requirements for activity. Biochim. Biophys. Acta **1462**, 29–54

42 Simmaco, M., Mignogna, G., Canofeni, S., Miele, R., Mangoni, M. L. and Barra, D. (1996) Temporins, antimicrobial peptides from the European red frog *Rana temporaria*. Eur. J. Biochem. **242**, 788–792

43 Srisailam, S., Arunkumar, A. I., Wang, W., Yu, C. and Chen, H. M. (2000) Conformational study of a custom antibacterial peptide cecropin B1: implications of the lytic activity. Biochim. Biophys. Acta **1479**, 275–285

44 Vogt, T. C. and Bechinger, B. (1999) The interactions of histidine-containing amphipathic helical peptide antibiotics with lipid bilayers. The effects of charges and pH. J. Biol. Chem. **274**, 29115–29121

45 Dathe, M. and Wieprecht, T. (1999) Structural features of helical antimicrobial peptides: their potential to modulate activity on model membranes and biological cells. Biochim. Biophys. Acta **1462**, 71–87

46 Sharon, M., Oren, Z., Shai, Y. and Anglister, J. (1999) 2D-NMR and ATR-FTIR study of the structure of a cell-selective diastereomer of melittin and its orientation in phospholipids. Biochemistry **38**, 15305–15316

47 Bechinger, B. (1996) Towards membrane protein design: pH-sensitive topology of histidine-containing polypeptides. J. Mol. Biol. **263**, 768–775

48 Bechinger, B. (1999) The structure, dynamics and orientation of antimicrobial peptides in membranes by multidimensional solid-state NMR spectroscopy. Biochim. Biophys. Acta **1462**, 157–183

49 Dempsey, C. E., Bazzo, R., Harvey, T. S., Syperek, I., Boheim, G. and Campbell, I. D. (1991) Contribution of proline-14 to the structure and actions of melittin. FEBS Lett. **281**, 240–244

50 Daly, J. W., Caceres, J., Moni, R. W., Gusovsky, F., Moos, M., Jr., Seamon, K. B., Milton, K. and Myers, C. W. (1992) Frog secretions and hunting magic in the upper Amazon: identification of a peptide that interacts with an adenosine receptor. Proc. Natl. Acad. Sci. U.S.A. **89**, 10960–10963

51 Steiner, H., Hultmark, D., Engstrom, A., Bennich, H. and Boman, H. G. (1981) Sequence and specificity of two antibacterial proteins involved in insect immunity. Nature (London) **292**, 246–248

52 Okada, M. and Natori, S. (1985) Primary structure of sarcotoxin I, an antibacterial protein induced in the hemolymph of *Sarcophaga peregrina* (flesh fly) larvae. J. Biol. Chem. **260**, 7174–7177

53 Simmaco, M., Mignogna, G., Barra, D. and Bossa, F. (1993) Novel antimicrobial peptides from skin secretion of the European frog *Rana esculenta*. FEBS Lett. **324**, 159–161

54 Habermann, E., Jentsch, J. and Hoppe Seylers, Z. (1967) Sequenzanalyse des melittins aus den tryptischen und peptischen spaltstuecken. Hoppe-Seyler's Z. Physiol. Chem. **348**, 37–50

Received 23 February 2001/25 May 2001; accepted 6 July 2001